Engineering Science and Technology, an International Journal 21 (2018) 727–735

HOSTED BY

Contents lists available at ScienceDirect

Engineering Science and Technology, an International Journal

journal homepage: www.elsevier.com/locate/jestch

Full Length Article

Numerical investigation of laminar convective heat transfer of graphene oxide/ethylene glycol-water nanofluids in a horizontal tube

Muhammad Sajjad [a,b,*], Muhammad Sajid Kamran [b], Rabia Shaukat [b], Mudather Ibrahim Mudather Zeinelabdeen [c]

[a] Department of Mechanical Engineering, Khwaja Fareed University of Engineering and Information Technology, Rahim Yar Khan 64200, Pakistan
[b] Faculty of Mechanical Engineering, University of Engineering and Technology, Lahore 54890, Pakistan
[c] School of Engineering and Materials Science, Queen Mary University of London, UK

ARTICLE INFO

Article history:
Received 14 December 2017
Revised 26 April 2018
Accepted 8 June 2018
Available online 19 June 2018

Keywords:
Graphene oxide nanofluids
Numerical analysis
Reynolds number
Heat transfer
Pressure drop

ABSTRACT

The study provides a numerical analysis of laminar forced convective heat transfer of graphene oxide nanosheets suspended in the mixture of water and ethylene glycol in laminar flow regime using single phase approach in a circular horizontal tube under constant heat flux conditions. The length and diameter of the simulation domain for numerical investigation are 2 m and 4.5 mm respectively. The effect of various flow conditions and weight concentrations have been investigated on local heat transfer coefficient, average heat transfer coefficient, friction factor, pressure drop and thermal performance factor of the nanofluids. The range of weight concentration and Reynolds number used in this study are 0.01–0.1 wt.% and 400–2000 respectively. The maximum percentage enhancement in average heat transfer coefficient was 13.04% for weight concentration and Reynolds number of 0.1 wt.% and 2000 respectively. The maximum pressure drop enhancement ratio was 2.12 at Reynolds number and weight concentration of 400 and 0.10 wt.%. The enhancement in heat transfer coefficient was found lower as compared to corresponding enhanced pressure drop for all weight concentrations. The thermal performance factor of nanofluids is less than one for all weight concentrations and nanofluids showed no advantage over base fluid as heat transfer fluid in laminar flow regime.

1. Introduction

Nanofluids are very important novel engineering fluids because of their possible utilization in various sectors. It has been observed that nanofluids can provide higher thermal performance as compare to conventional thermal fluids such as water and ethylene glycol. So, there exists a strong possibility to improve the performance of thermal systems by using these engineering fluids.

Nanofluids have been tried for various applications including solar thermal systems [1], refrigeration systems as nano-refrigerant [2], vehicle cooling systems [3], electronic cooling systems [4], medical applications [5], lubrication systems [6], fuel cell cooling systems [7], hydraulic braking systems [8], combustion systems [9] and etc. The further details about the investigations on various kinds of nanofluids and their applications can be found in [10–14].

Nanofluid basically consist of two main components i.e. nanomaterial and the base fluid. There are number of ways to prepare the nanofluids either by mixing one or two kinds of nanomaterials in one or two types of base fluids (e.g. base fluid obtained by the combination of water and ethylene glycol). Nanomaterials can be obtained from metals (Al, Cu, Fe), metal oxides (Al_2O_3, TiO_2, CuO, Fe_3O_4), semiconductors (Cu_2O) or from non-metals (ND, CNT, GNP, GO). In a recent study, Mohebbi et al. [15] simulated forced convective heat transfer of water based three metal oxide (CuO, Al_2O_3, TiO_2) nanofluids using lattice Boltzmann method at very low Reynolds number (Re = 10–70) in a channel with extended surfaces. The increase in height of extended surfaces resulted enhancement in Nusselt number and this enhancement was higher for CuO nanofluids as compare to other two nanofluids. Alawi et al. [16] investigated the effect of nanoparticle shape, temperature and volume concentrations on viscosity and thermal conductivity of SiO_2, Al_2O_3, ZnO and CuO nanofluids using Koo and Kleinstreuer Model. They found that temperature has significant effect on

* Corresponding author at: Department of Mechanical Engineering, Khwaja Fareed University of Engineering and Information Technology, Rahim Yar Khan 64200, Pakistan.
E-mail addresses: muhammad.sajjad@kfueit.edu.pk (M. Sajjad), m.s.kamran@uet.edu.pk (M.S. Kamran).

Peer review under responsibility of Karabuk University.

https://doi.org/10.1016/j.jestch.2018.06.009
2215-0986/

Nomenclature

A, B, C	Correlation coefficients
C_p	Specific heat, J/kg K
D	Diameter of the channel, m
f_d	Darcy friction factor
h_{ave}	Average heat transfer coefficient, W/m^2 K
$h_{ave,\ e}$	Average heat transfer coefficient enhancement (%)
h_x	Local heat transfer coefficient, W/m^2 K
$h_{x,\ e}$	Local heat transfer coefficient enhancement (%)
L	Length of tube, m
N_x	Number of mesh elements in radial direction
N_y	Number of mesh elements in axial direction
P	Pressure, Pa
ΔP	Pressure drop, Pa
P_e	Pressure drop enhancement ratio, $\Delta P_f/\Delta P_b$
q''	Heat flux, W/m^2
Re	Reynolds number, Re = $\rho\ \bar{V}D/\mu$
r	radius of the channel, m
T	Temperature, K
V	Velocity of the fluid, m/s
$\overline{V}$	Average velocity of the fluid, m/s
x	Cartesian coordinate in axial direction, m
y	Cartesian coordinate in radial direction, m

Greek symbols

ρ	Density, kg/m^3
μ	Dynamic viscosity, Pa s
ϕ	Concentration of nanomaterial
k	Thermal conductivity, W/m K

Subscripts

a	Bulk (temperature)
b	Base fluid
f	Nanofluid
m	Weight (concentration)
s	Solid nanomaterial
v	Volume (concentration)
w	wall

Acronyms

CNT	Carbon nanotubes
EG	Ethylene glycol
G	Glycerol
GNP	Graphene nanoplatelets
GO	Graphene oxide nanosheets
MWCNT	Multi-walled carbon nanotubes
ND	Nano-diamond
PF	Performance factor
SIMPLE	Semi Implicit Method for Pressure Linked Equations
W	Water

viscosity of nanofluids and it decreases with the increase in temperature. However, an increase in thermal conductivity was found with the increase in temperature. While increased particle loading resulted in the enhancement of both viscosity and the thermal conductivity.

The distinct thermophysical properties of the graphene have made it strong candidate for various applications including thermal systems since the initial investigations of Novoselov et al. [17]. Yu et al. [18] experimentally investigated the augmentation in thermal conductivity of ethylene glycol based nanofluids having GO nanosheets and observed 61% increase in thermal conductivity at volume concentration of 5%. Meyer et al. [19] investigated the heat transfer and flow characteristics of water based nanofluids containing MWCNT for laminar, transitional and turbulent flow (Re = 1000–8000) regime in horizontal tube under constant heat flux of 13000 W/m^2 and at volume concentrations of 0.33%, 0.75% and 1.0% respectively. It was found that the friction factor of nanofluids were less than distilled water in laminar flow regime at same Reynolds number. They found that the enhancement in viscosity was more than four times of thermal conductivity which resulted in enhanced pumping requirements. They concluded that the water based MWCNT may provide no benefit over base fluid due to enhanced pressure losses in laminar flow regime. Ijam et al. [20] analysed the effect of temperature and particle loading on improvement in thermal conductivity of GO/EG-W nanofluids. A maximum enhancement of 11.7% was found in thermal conductivity at nanosheet loading and temperature of 0.1 wt.% and 318.15 K respectively. Sadeghinezhad et al. [21] observed significant improvement in convective heat transfer coefficient up to 160% with maximum enhancement of 14.6% in pressure loss for the turbulent flow of water based GNP nanofluids in horizontal tube. Heyhat et al. [22] performed experimentation to determine the augmentation in thermal conductivity of reduced GO/EG nanofluids for various controlling parameters including nanomaterial concentration and nanofluids temperature. The percentage enhancement in thermal conductivity was found to be 16.32% at weight concentration of 0.05%.

Kimiagar et al. [23] studied the effect of nanosheets concentration and temperature on thermal conductivity of reduced GO nanosheets dispersed in ethylene glycol. It was found that reduced GO/EG nanofluids provided maximum enhancement of 17.8% in thermal conductivity at weight concentration and temperature of 0.05 wt.% and 328.15 K respectively. Cabaleiro et al. [24] comprehensively investigated the thermophysical properties of GNP/EG-W nanofluids and obtained correlations for density, viscosity and thermal conductivity of nanofluids. They also observed that there may be no significant improvements in heat transfer of GNP/EG-W nanofluids over the base fluid and rather it will enhance pumping requirements. Ranjbarzadeh et al. [25] studied the heat transfer and flow features of GO/W nanofluids in copper tubes covered by cross flow of air behaving as heat exchanger. They concluded that the maximum increase in Nusselt number and friction factor was 51.4% and 21% respectively at nanofluids volume concentration and Reynolds number of 0.2% and 3250 respectively. In another study, Ranjbarzadeh et al. [26] experimentally investigated the heat transfer intensification for turbulent flow of water based GO nanofluids in circular shape channel under isothermal conditions with volume concentrations and Reynolds number of 0.025–0.1% and 5250 & 36,500 respectively. It was found that the highest enhancement in convective heat transfer coefficient and pressure drop were 40.3% and 16% respectively at tested conditions.

Yazid et al. [27] comprehensively reviewed the application of various kinds of nanofluids with CNT as base fluid in heat and mass transfer applications for different channels such as straight tubes and heat exchangers. They also discussed various equations to assess the thermohydraulic performance of nanofluids. It was concluded that the pressure drop and pumping power is enhanced with the addition of nanoparticles in base fluid however their effect can be minimized by maintaining low concentration of nanofluids. The covalent functionalization technique was

recommended for the preparation of CNT based nanofluids in order to achieve higher stability. Sidik et al. [28] extensively reviewed the research studies, conducted to analyse the potential utilization of CNT nanofluids in solar collector applications as solar energy harvesting fluid. They also discussed the preparation techniques and effect of various factors on thermal conductivity of CNT based nanofluids. Moreover, various challenges for the practical utilization of CNT nanofluids were also comprehensively considered. In a very recent study, Ettefaghi et al. [29] investigated thermal conductivity and convective heat transfer coefficient of a new kind of nanofluid, prepared by mixing Carbon quantum dot nanoparticles in car radiator coolant at weight concentrations of 0%, 0.01%, 0.02%, 0.05% and 1.0% respectively. The highest enhancement in heat transfer coefficient was 16.2% at weight concentration and Reynolds number of 0.2% and 3249 respectively. Meyer and Everts [30] performed experimental investigations on heat transfer performance of water for two different test sections (4 mm and 11.5 mm) at various heat flux conditions (1–8 KW/m^2). They observed that the free convection effects were 24 times less in the 4 mm test section as compare to 11.5 mm test section, as Grashof number varies directly proportional to cube of tube diameter. They observed that the free convection effects increased along the tube length, causing Nusselt numbers to increase. They also found that, deviation from forced convection line increased with the increase in heat flux, due to enhanced free convection effects.

It can be seen that a limited number of research studies are available in literature for the investigation of thermohydraulic characteristics of GO/EG-W nanofluids. So, there is need to further analyse the nanofluids containing graphene oxide as nanomaterial. In present research work, numerical investigations have been performed for the analysis of heat transfer and flow features of GO/EG-W nanofluids.

2. Mathematical formulation

The details of the mathematical modelling involved in numerical investigations are given below:

2.1. Physical model and boundary conditions

Fig. 1 represents the computational domain used for the numerical analysis of GO/EG-W nanofluids. The inlet velocity profile was laminar and hydro-dynamically fully developed. A uniform temperature profile (T = 298.15 K) at inlet and uniform heat flux on the wall were applied as thermal boundary conditions. The length and radius of the physical domain are 2.0 m and 2.25 mm respectively.

2.2. Governing equations

There are various methods to analyse the thermal performance of nanofluids including single phase and the two-phase approaches. Albojamal and Vafai [31] concluded that the single phase approach is preferable at low concentrations for the analysis of nanofluids because of its less computational cost. Their conclusions were based on comprehensive investigations and numerical results of single-phase approach and two-phase approach were compared with the experimental data available in literature. As in current study, the concentration of nanomaterial is low, so the numerical analysis of heat transfer and flow characteristics of GO/EG-W was performed using single phase approach and the relevant governing equations including continuity, momentum and energy equation are given by Eqs. (1)–(3) respectively [32].

$$\nabla \cdot (\rho \vec{V}) = 0 \tag{1}$$

$$\nabla \cdot (\rho \vec{V}\vec{V}) = -\nabla(P) + \nabla \cdot (\mu \nabla \vec{V}) \tag{2}$$

$$\nabla \cdot (\rho \vec{V} C_p T) = \nabla \cdot (k \nabla T) \tag{3}$$

3. Thermophysical properties of GO/EG-W nanofluids

The temperature dependent thermophysical properties of the GO/EG-W (40:60) nanofluids were derived from experimental data of Ijam et al. [33] in order to perform numerical investigations. The detail description of the thermophysical properties is given below:

3.1. Density

The most commonly used correlation for the estimation of density is given by Eq. (4) [34,35].

$$\rho_f = \phi_v \rho_s + (1 - \phi_v)\rho_b \tag{4}$$

However, Eq. (4) provides approximate results for the density of nanofluids because one correlation may not provide reasonable results for each kind of nanofluid. So, it will be preferable to utilize experimental data for the calculation of density of nanofluids. The correlation for the density of nanofluids is given by Eq. (5), which is valid for temperature and nanosheets concentration of 298.15 K to 318.15 K and 0.01 wt.% to 0.1 wt.% respectively. The coefficients A and B are given in Table 1.

$$\rho_f = A + BT \tag{5}$$

3.2. Specific heat

Two methods have been adopted by the researchers to calculate specific heat capacity of the nanofluids as given by Eqs. (6) [35] and (7) [13].

$$C_{p,f} = \phi_v C_{p,s} + (1 - \phi_v) C_{p,b} \tag{6}$$

$$(\rho C_p)_f = \phi_v (\rho C_p)_s + (1 - \phi_v)(\rho C_p)_b \tag{7}$$

For GO/EG-W nanofluid, both Eqs. (6) and (7) [34] over predict the specific heat of nanofluids as shown by Ijam et al. [33]. The Eq. (8) provides correlation to estimate the specific heat of the nanofluids and Table 2 shows the relevant parameters.

$$C_{p,f} = A + BT \tag{8}$$

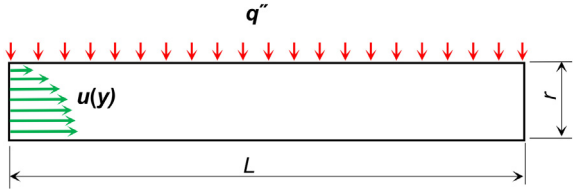

Fig. 1. Computational domain used for the numerical investigations.

Table 1
Values of correlation coefficients for the density of GO/EG-W nanofluids.

ϕ_m (%)	A	B
0.00	1203.8935	−0.49
0.01	1198.1435	−0.49
0.05	1206.638	−0.52
0.07	1191.312	−0.48
0.10	1171.323	−0.42

Table 2
Values of correlation coefficients for the specific heat capacity of GO/EG-W nanofluids.

ϕ_m (%)	A	B
0.00	2547.2585	3.21
0.01	2287.728	4.28
0.05	2100.389	5.14
0.07	2240.9655	4.03
0.10	1989.6015	3.99

3.3. Thermal conductivity

The thermal conductivity was calculated using Eq. (9). The corresponding values of coefficient A and B are given in Table 3 against various weight concentrations of nanofluids.

$$k_f = A + BT \tag{9}$$

3.4. Viscosity

Viscosity is an important thermophysical property to be determined. There are number of correlations which are available in literature to estimate the viscosity of the nanofluids [36] but none of them is valid for all type of nanofluids. The following polynomial correlation given by Eq. (10) was developed on the basis of data provided in [33]. The coefficients involved in Eq. (10) have been given in Table 4 at various weight concentrations of GO/EG-W nanofluids.

$$\mu_f = A - BT + CT^2 \tag{10}$$

The thermo-physical properties of water – ethylene glycol (60:40) mixture were validated by comparing the calculated values from the correlations with the ASHRAE reference [37] values as given in Table 5. The maximum errors in density and specific heat capacity, thermal conductivity and viscosity are 0.03%, 0.5%, 4% and 1.5% respectively.

4. Numerical investigations

The numerical investigations were performed using Fluent 14.0. The governing equations including mass, momentum and energy equation were solved using finite volume method. The second order upwind scheme was implemented for the solution of momentum and energy terms. Similarly, pressure terms were solved using standard method and pressure velocity coupling was solved using SIMPLE method. The residuals were converged to below 10^{-6}.

Table 3
Values of correlation coefficients for the thermal conductivity of GO/EG-W nanofluids.

ϕ_m (%).	A	B
0.00	0.18531	0.0008
0.01	0.175584	0.00084
0.05	0.117421	0.00106
0.07	0.0474605	0.00133
0.10	0.007375	0.0015

Table 4
Values of correlation coefficients for the viscosity of GO/EG-W nanofluids.

ϕ_m (%)	A	B	C
0.00	0.095876843	−0.000562567	$8.36789841 \times 10^{-7}$
0.01	0.097576223	−0.000569715	$8.42930733 \times 10^{-7}$
0.05	0.103702195	−0.000606736	$9.00218584 \times 10^{-7}$
0.07	0.098296592	−0.000568389	$8.36483053 \times 10^{-7}$
0.10	0.092691001	−0.000528819	$7.70959661 \times 10^{-7}$

The local and average convective heat transfer coefficients were calculated using Eqs. (11) and (12).

$$h_x = \frac{q}{[T_w - T_a]_x} \tag{11}$$

$$h_{ave} = \frac{1}{L}\int_0^L h_x dx \tag{12}$$

The theoretical friction factor can be calculated using Hagen–Poiseuille equation as given by Eq. (13).

$$f_d = \frac{64}{\mathrm{Re}} \tag{13}$$

4.1. Mesh convergence

The mesh convergence study was performed by testing various grid sizes, with nonuniform distribution in radial and axial directions. The temperature curves gradually became close as the mesh size was increased. Fig. 2 provides the temperature profile at center line of the channel for pure water at Reynolds number, Re = 1200 and Prandtl number, Pr = 5.4 for different grid sizes. Higher grid density was kept near the wall where gradient was very high. The mesh sizes of 18 × 1440 and 20 × 1600 provides insignificant difference in corresponding temperature profiles. So, the fine mesh size of 18 × 1440 (i.e. 18 nodes in radial direction and 1440 nodes in axial direction) was selected for numerical investigations in order to reduce computational time with justified accuracy.

4.2. Model validation

One of the key step for the numerical analysis is to validate the numerical model by comparing the simulation results with known experimental or theoretical results. The Fig. 3 shows comparison of local Nusselt number profile in horizontal tube with experimental and theoretical results of Meyer and Everts [30] and Churchill and Ozoe [38] for hydrodynamically and thermally developing flow. The temperature dependent thermophysical properties of water were obtained from the correlations developed by Popiel and Wojtkowiak [39]. It is clear from Fig. 3 that there is good agreement among numerical, experimental and theoretical results. The average deviation of numerical results from experimental results of Meyer and Everts [30] is 6.48%.

To improve the validity, a comparison of local heat transfer coefficient was made with experimental data of Meyer et al. [19] at same conditions for volume concentration of 0.33% as depicted by Fig. 4. Meyer et al. [19] analysed laminar convective heat transfer and flow characteristics of water based MWCNT nanofluids in horizontal tube with circular cross-section under constant heat flux boundary conditions. The temperature dependent properties of the water based MWCNT nanofluids were considered for validation purpose which are given by Eqs. (14) and (15).

$$\mu_f = (1 + 60\phi_v)\mu_b \tag{14}$$

$$k_f = (1 + 7\phi_v)k_b \tag{15}$$

While density and specific heat capacity of MWCNT were taken 2100 kg/m^3 and 470 kJ/kg K respectively as reported by Garbadeen et al. [40].

It can be seen from Fig. 4, that the present numerical results are in good agreement with the experimental results of Meyer et al. [19]. The deviation between experimental and numerical results increased after x/D = 120, as experimental Nusselt number slightly increased due to possible use of bell-mouth inlet instead of

Table 5
Comparison of thermo-physical properties of base fluid with ASHRAE [37] reference data.

	Correlations			ASHRAE [37]		
T	25 °C	30 °C	40 °C	25 °C	30 °C	40 °C
ρ	1057.9	1055.4	1050.6	1057.6	1055.39	1050.62
Cp	3504.4	3520.4	3552.5	3485	3518	3535
k	0.4238	0.4278	0.4358	0.408	0.412	0.419
μ	0.00253	0.00224	0.00177	0.00257	0.00226	0.00177

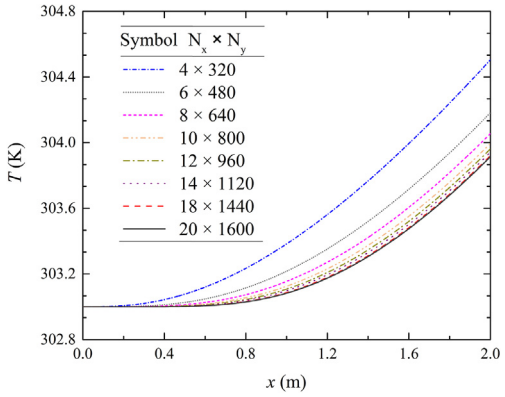

Fig. 2. Axial temperature profile at center line of the channel for water.

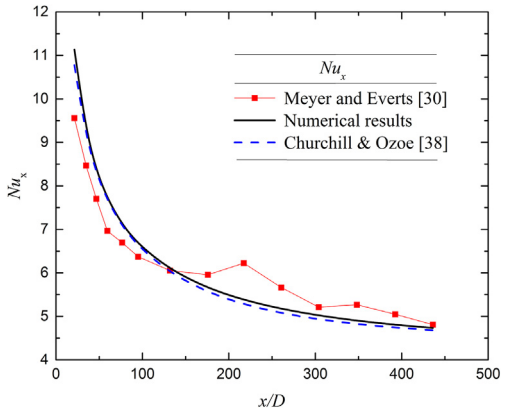

Fig. 3. Comparison of numerical results with corresponding experimental and theoretical results for local Nusselt number for water at Re = 1800 and q_w = 3000 W/m^2.

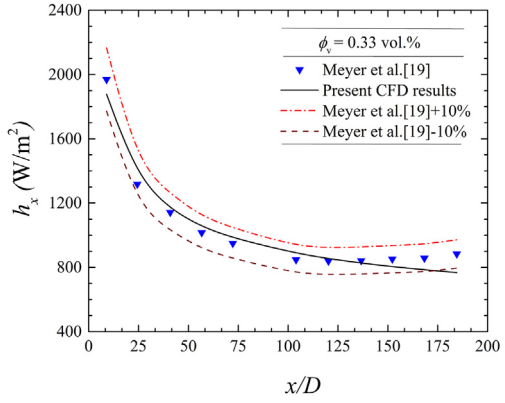

Fig. 4. Comparison of local heat transfer coefficient for MWCNT at Re = 2000, volume concentration of 0.33% under heat flux of 13 KW/m^2 with experimental results of Meyer et al. [19].

square-edged inlet as reported by Meyer et al. [19]. The percentage difference between experimental and numerical results was 7% at ~x/D = 9.3 and 13% at ~x/D = 185. However, average deviation of numerical results from experimental results was 4.8%.

4.3. Results

The numerical analysis of the convective heat transfer coefficient and pressure drop was carried out using single phase approach. The discussion on flow and heat transfer analysis is given in next section.

4.3.1. Pressure drop and friction factor results

The comparison for the pressure drop of nanofluids with base fluid provides indication about the pumping power requirements. It was found that if higher is the Reynolds number then higher will be the pressure loss for both the base fluid and the nanofluid as given in Fig. 5. The qualitative analysis of the Fig. 5 reveals that the increasing trend of pressure loss is similar for all weight concentrations of GO/EG-W nanofluids. At weight concentration of 0.1 wt.% and Re = 2000, the pressure drop was observed to be the highest and its value was 16183.3 Pa among all studied conditions.

The pressure drop was also increased with the increase in weight concentration perhaps because of higher viscosity of the GO/EG-W nanofluids as shown in Fig. 6. The higher viscosity of the nanofluids is due to the addition of nanosheets in base fluid which results in more pressure drop. For example, at Reynolds number of 1600, the pressure drop was enhanced from 6903.4 Pa to 12872.5 Pa, when weight concentration was varied from 0.01 wt.% to 0.1 wt.% as depicted in Fig. 6.

The effect of Reynolds number on enhancement ratio of pressure drop can be analysed from Fig. 7. It can be seen from Fig. 7 that at low weight concentrations (e.g. 0.01 wt.%), the effect of Reynolds number is less on pressure drop enhancement ratio. However, at higher weight concentrations such as at 0.1 wt.%, the pressure drop enhancement ratio is decreasing with the increase in Reynolds number. The highest value of pressure drop enhancement ratio was 2.12 at Re = 400 and weight concentration of 0.1 wt.%.

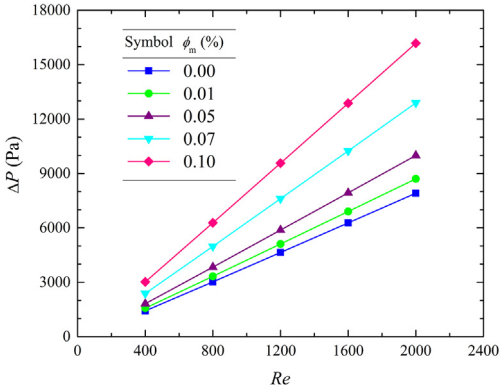

Fig. 5. Effect of Reynolds number on pressure drop for various weight concentrations.

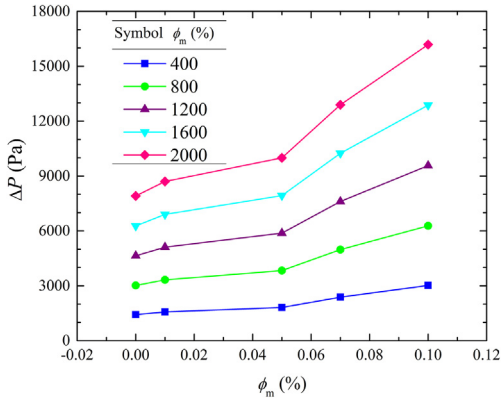

Fig. 6. Variation in pressure drop with weight concentrations at different Reynolds numbers.

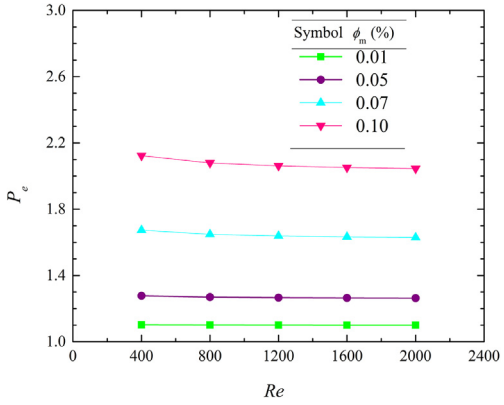

Fig. 7. Effect of Reynolds number on pressure drop enhancement for various weight concentrations.

The friction factor of both nanofluids and the base fluid decreases with the increase in Reynolds number for all weight concentrations and there is no significant enhancement in friction factor with the increase in weight concentrations as shown in Fig. 8.

4.3.2. Local convective heat transfer coefficient results

In order to study the heat transfer characteristics of GO/EG-W nanofluids, variation in local heat transfer coefficient was investigated with axial dimension as described by Fig. 9. It can be observed from Fig. 9 that as the nanofluids concentration is being

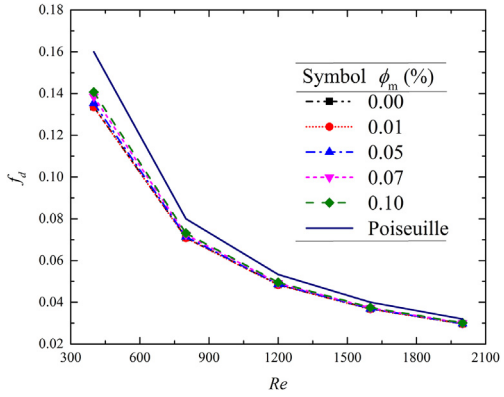

Fig. 8. Effect of Reynolds number on friction factor at various weight concentrations.

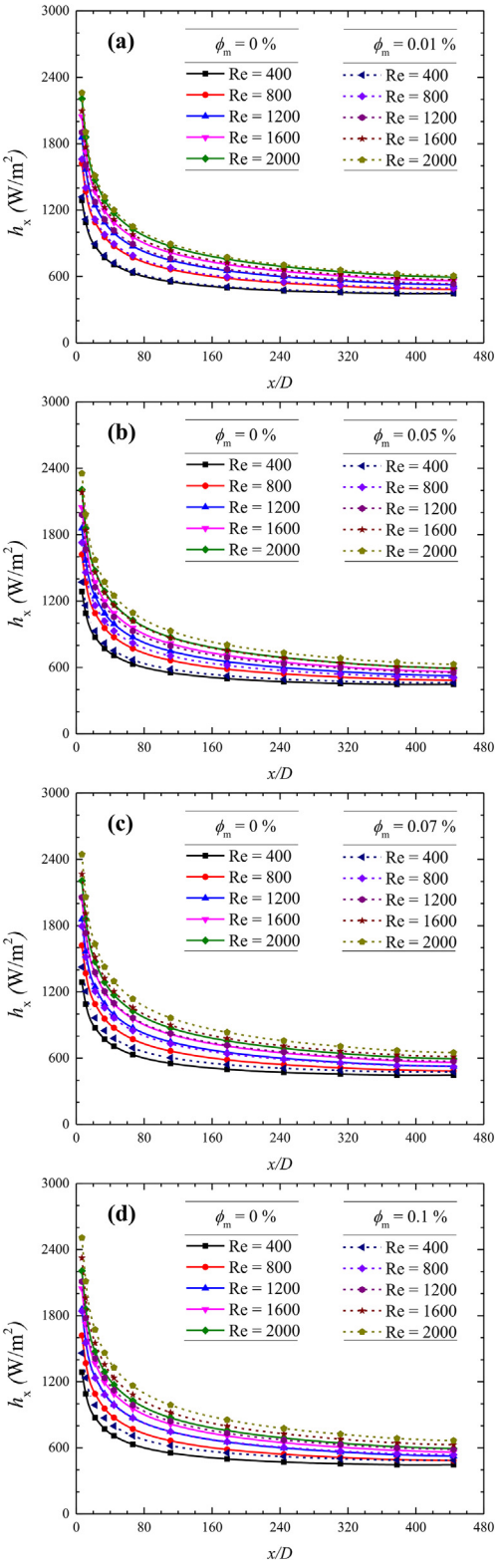

Fig. 9. Heat transfer coefficient variation with axial dimensionless distance at various weight concentrations and flow conditions.

increased, the local heat transfer coefficient is also being improved for the studied range of Reynolds number. For example, at Re = 400 and x/D = 66.67, the local convective heat transfer coefficient is increased from 645.2 W/m^2 K to 709.7 W/m^2 K for weight concentration of 0.01 wt.% and 0.1 wt.% respectively as given in Fig. 9(a) and (d).

Similarly, the local heat transfer coefficient was increased from 1052 W/m^2 K to 1163.8 W/m^2 K when weight concentration was changed from 0.01 wt.% to 0.1 wt.% at axial dimensionless distance and Reynolds number of 66.67 and 2000 respectively. A similar trend was observed for all other flow conditions as expressed in Fig. 9.

The local heat transfer coefficient is also increasing with the increase in weight concentration at entrance region of the tube as shown in Fig. 9. It is also clear from Fig. 9 that the enhancement in local heat transfer coefficient is higher at entrance region of the channel at all values of Reynolds number (400–2000). Fig. 9 also represents the effect of Reynolds number on local convective heat transfer coefficient of GO/EG-W nanofluids. The enhancement in Reynolds number results in the enhancement of local heat transfer coefficient for all values of nanosheets concentrations. It can be easily shown that at nanosheets concentration of 0.1 wt.%, the local heat transfer coefficient of nanofluids at entrance region (x/D = 66.7) was increased from 709.7 W/m^2 K to 1163.8 W/m^2 K when Reynolds number was increased from 400 to 2000 respectively as shown in Fig. 9(d).

The augmentation in local heat transfer coefficient with Reynolds number at entrance region of the channel can also be seen from Fig. 10. The local heat transfer coefficient is having lower values at Re = 400 and higher values at Re = 2000 for all weight concentrations. It is clear from the Fig. 10 that, higher value of the Reynolds number is having positive effect on heat transfer coefficient. It means, that the nanofluids may provide better performance at higher Reynolds numbers. The variation of local heat transfer coefficient with GO nanosheets concentrations at x/D = 66.7 can be seen in Fig. 11.

The Fig. 12 exhibits the percentage augmentation in local heat transfer coefficient when plotted against Reynolds number. The percentage augmentation in heat transfer coefficient was also increased with the increase in Reynolds number. For example, percentage enhancement in local heat transfer coefficient at entrance region was 9.7% at weight concentration and Reynolds number of 0.07 wt.% and 400 respectively. The percentage enhancement in heat transfer coefficient was reached to 10.5% at Re = 2000 while keeping other parameters same. The highest percentage augmentation in local heat transfer coefficient was 13.2% at Reynolds number and weight concentration of 2000 and 0.1 wt.% respectively.

4.3.3. Average convective heat transfer coefficient results

Fig. 13 shows the relationship between Reynolds number and average heat transfer coefficient at heat flux of 3500 W/m^2 for weight concentration from 0.01 wt.% to 0.1 wt.% of GNO/EG-W nanofluid. The graph shows that the average heat transfer coefficient increases as Reynolds number is increases. The maximum

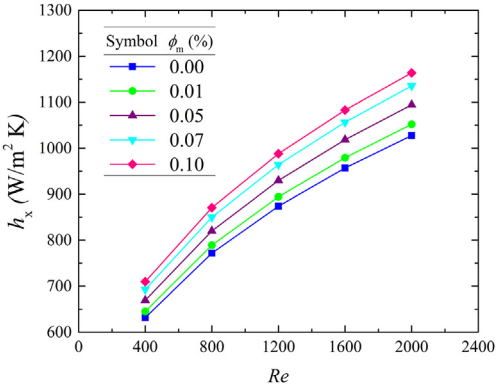

Fig. 10. Variation of local heat transfer coefficient with Reynolds number (x/D = 66.7).

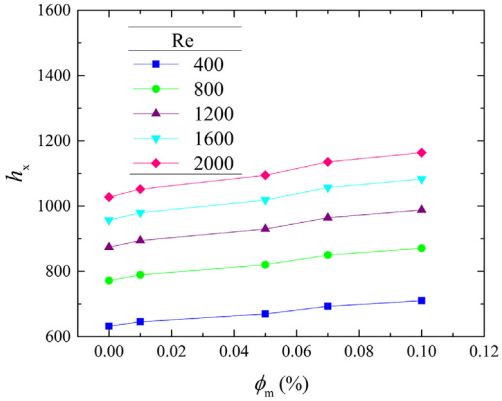

Fig. 11. Effect of weight concentration on local heat transfer coefficient (x/D = 66.7).

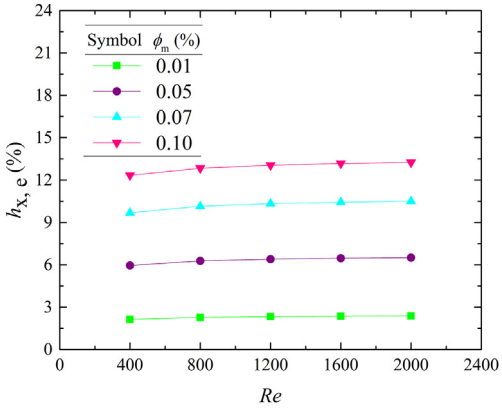

Fig. 12. Percentage increment in local heat transfer coefficient with Reynolds number (x/D = 66.7).

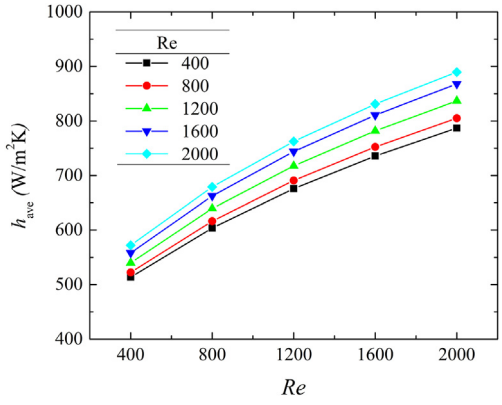

Fig. 13. Variation of average heat transfer coefficient with Reynolds number.

percentage enhancement in average heat transfer coefficient was 11.41%, 12.5%, 12.82%, 12.96% and 13.04% at Reynolds numbers of 400, 800, 1200, 1600 and 2000 respectively for weight concentration of 0.1 wt.% as depicted by Fig. 14.

The average heat transfer coefficient also increases with the increase in nanosheets concentration as shown in Fig. 15. For example, at Re = 2000, the enhancement in heat transfer coefficient was 2.3%, 6.33%, 10.28% and 13.04% for weight concentration of 0.01 wt.%, 0.05 wt.%, 0.07 wt.% and 0.1 wt.% respectively. The increase of heat transfer coefficient was highest (889.51 W/m^2) at higher Reynolds numbers (Re = 2000) and at higher concentra-

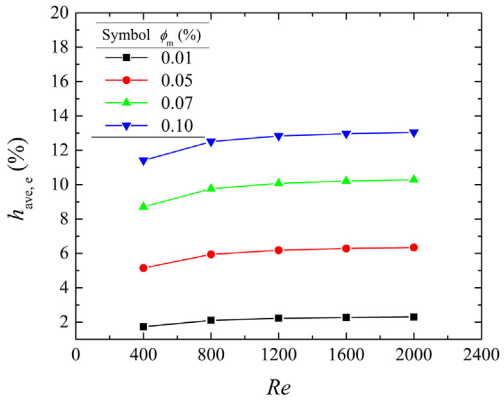

Fig. 14. Variation of percentage enhancement in average heat transfer coefficient for different flow conditions at various weight concentrations.

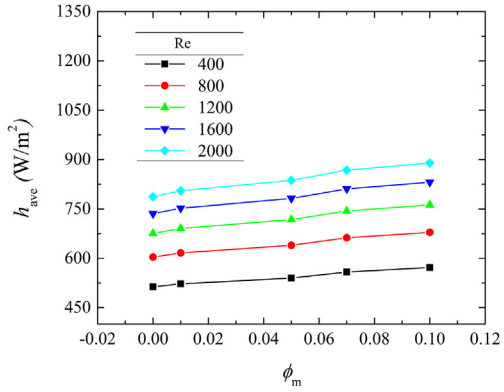

Fig. 15. Variation of average heat transfer coefficient for different flow conditions at various weight concentrations.

tion (0.1 wt.%). Ghozatloo et al. [41] observed 35.6% enhancement in heat transfer coefficient for water-based graphene nanofluids at Reynolds number of 1940, weight concentration of 0.1 wt.% at 38 °C in shell and tube heat exchanger. Arzani et al. [42] found 22% improvement in heat transfer coefficient at weight concentration of 0.1 wt.% in turbulent flow regime for water based GNP nanofluids. However, in present study the maximum enhancement in average heat transfer coefficient is 13.04%.

4.3.4. Thermal-hydraulic performance

The thermo-physical properties of the base fluid are modified when nano-sized solid particles are added in the base fluid using particular mixing technique. The thermal conductivity of the resulting nanofluids is greater than that of base fluid which is due to the presence of solid particles having higher thermal conductivity as compared to base fluid. However, viscosity of the nanofluid will also be higher as compare to base fluid which will result in the increase of pressure drop of nanofluid as compare to the base fluid. Hence, it is very important to describe the effect of both fluid properties such as the enhanced viscosity of the nanofluid along with the enhanced thermal conductivity. To simultaneously analyse the effect of enhanced viscosity and enhanced thermal conductivity of nanofluids, thermal performance factor of nanofluids was calculated using Eq. (16) [43].

$$PF = \frac{(h_f/h_b)}{(\Delta P_f/\Delta P_b)} \tag{16}$$

The thermal performance factor basically compares the enhancement ratio of the heat transfer coefficient with the

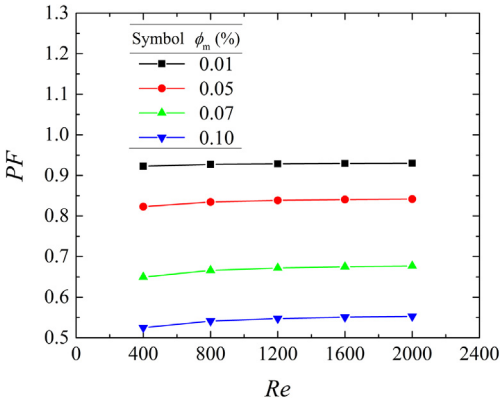

Fig. 16. Thermal performance factor of nanofluids.

enhancement ratio of pressure drop. If the value of thermal performance factor is more than one, then the use of nanofluid will be beneficial otherwise there will be no advantage. Fig. 16 shows thermal performance of GO/EG-W nanofluids at various weight concentrations in laminar flow regime. The performance factor of GO/EG-W nanofluids is less than one at all weight concentrations. It means nanofluids seems to provide no advantage over base fluid as thermal fluid in laminar flow regime. Meyer et al. [19] also made similar findings for water based MWCNT nanofluids.

5. Conclusion

The effect of Reynolds number and weight concentrations was studied on flow and heat transfer characteristics of GO/EG-W nanofluids considering temperature dependent properties in horizontal straight tube under constant heat flux boundary conditions. On the basis of discussion made in Section 4.3, following important conclusions have been made:

- Pressure drop increased both with the increase in Reynolds number and weight concentration. The enhancement in pressure drop increased with the increase in concentration but decreased with the increase in Reynolds number for all cases considered. The highest value of pressure drop enhancement ratio was 2.12 at weight concentrations of 0.1 wt.% and Re = 400.
- The enhancement in local heat transfer coefficient is more prominent in the entrance region of the selected channel as proved from the discussion in Section 4.3.
- The average and local heat transfer coefficients of nanofluid were higher as compare to base fluid in all cases. The enhancement in local heat transfer coefficient increased both with the increase in Reynolds number and weight concentration of GO nanosheets. The highest percentage increase in local convective heat transfer coefficient was 13.2% at entrance region of the tube at Reynolds number and weight concentration of 2000 and 0.1 wt.% respectively. The maximum enhancement in average heat transfer coefficient was 13.04% at Re = 2000 and weight concentration of 0.1 wt.% respectively.
- The performance factor of the studied nanofluids was less than one for all cases. This was because of the fact that the heat transfer coefficient enhancement was less as compare to pressure drop enhancement. The highest value of thermal performance factor was 0.93 at Reynolds number, Re = 2000 and particle loading of 0.01 wt.%.

Hence, it can be concluded that GO/EG-W nanofluid analysed in this study seems to have no advantage over the base fluid as ther-

mal fluid in laminar flow regime under constant heat flux boundary conditions.

References

[1] D.R. Rajendran, E.G. Sundaram, P. Jawahar, Experimental studies on the thermal performance of a parabolic dish solar receiver with the heat transfer fluids SiC + water nano fluid and water, J. Therm. Sci. 26 (2017) 263–272.

[2] S.S. Sanukrishna, A.S. Vishnu, M. Jose Prakash, Nanorefrigerants for energy efficient refrigeration systems, J. Mech. Sci. Technol. 31 (2017) 3993–4001.

[3] A.M. Hussein, K. Kadirgama, K.V. Sharma, D. Ramasamy, R.A. Bakar, Heat transfer enhancement with nanofluids for automotive cooling, in: V.S. Korada, N. Hisham, B. Hamid (Eds.), Engineering Applications of Nanotechnology: From Energy to Drug Delivery, Springer International Publishing, Cham, 2017, p. 100.

[4] J.R. Bose, N. Ahammed, L.G. Asirvatham, Thermal performance of a vapor chamber for electronic cooling applications, J. Mech. Sci. Technol. 31 (2017) 1995–2003.

[5] L. Valdés, D. Hernández, L.C. de Ménorval, I. Pérez, E. Altshuler, J.O. Fossum, et al., Incorporation of tramadol drug into Li-fluorohectorite clay: a preliminary study of a medical nanofluid, Eur. Phys. J. Special Topics 225 (2016) 767–771.

[6] M. Shabgard, M. Seyedzavvar, M. Mohammadpourfard, Experimental investigation into lubrication properties and mechanism of vegetable-based CuO nanofluid in MQL grinding, Int. J. Adv. Manuf. Technol. (2017). May 05.

[7] M.R. Islam, B. Shabani, G. Rosengarten, J. Andrews, The potential of using nanofluids in PEM fuel cell cooling systems: a review, Renew. Sustain. Energy Rev. 48 (2015) 523–539.

[8] M.J. Kao, C.H. Lo, T.T. Tsung, Y.Y. Wu, C.S. Jwo, H.M. Lin, Copper-oxide brake nanofluid manufactured using arc-submerged nanoparticle synthesis system, J. Alloy. Compd. 434 (2007) 672–674.

[9] H. Venu, V. Madhavan, Effect of nano additives (titanium and zirconium oxides) and diethyl ether on biodiesel-ethanol fuelled CI engine, J. Mech. Sci. Technol. 30 (2016) 2361–2368.

[10] L. Yang, Y. Hu, Toward TiO2 nanofluids—part 2: applications and challenges, Nanoscale Res. Lett. 12 (2017) 446.

[11] A. Kumar, S. Subudhi, Preparation, characteristics, convection and applications of magnetic nanofluids: a review, Heat Mass Transf. (2017).

[12] S. Senthilraja, M. Karthikeyan, R. Gangadevi, Nanofluid applications in future automobiles: comprehensive review of existing data, Nano-Micro Lett. 2 (2010) 306–310.

[13] S.A. Angayarkanni, J. Philip, Review on thermal properties of nanofluids: recent developments, Adv. Colloid Interface Sci. 225 (2015) 146–176.

[14] M. Raja, R. Vijayan, P. Dineshkumar, M. Venkatesan, Review on nanofluids characterization, heat transfer characteristics and applications, Renew. Sustain. Energy Rev. 64 (2016) 163–173.

[15] R. Mohebbi, M.M. Rashidi, M. Izadi, N.A.C. Sidik, H.W. Xian, Forced convection of nanofluids in an extended surfaces channel using lattice Boltzmann method, Int. J. Heat Mass Transf. 117 (2018) 1291–1303.

[16] O.A. Alawi, N.A.C. Sidik, H.W. Xian, T.H. Kean, S.N. Kazi, Thermal conductivity and viscosity models of metallic oxides nanofluids, Int. J. Heat Mass Transf. 116 (2018) 1314–1325.

[17] K.S. Novoselov, A.K. Geim, S.V. Morozov, D. Jiang, Y. Zhang, S.V. Dubonos, et al., Electric field effect in atomically thin carbon films, Science 306 (2004) 666–669.

[18] Y. Wei, X. Huaqing, B. Dan, Enhanced thermal conductivities of nanofluids containing graphene oxide nanosheets, Nanotechnology 21 (2010) 055705.

[19] J.P. Meyer, T.J. McKrell, K. Grote, The influence of multi-walled carbon nanotubes on single-phase heat transfer and pressure drop characteristics in the transitional flow regime of smooth tubes, Int. J. Heat Mass Transf. 58 (2013) 597–609.

[20] A. Ijam, A. Moradi Golsheikh, R. Saidur, P. Ganesan, A glycerol–water-based nanofluid containing graphene oxide nanosheets, J. Mater. Sci. 49 (2014) 5934–5944.

[21] E. Sadeghinezhad, M. Mehrali, S. Tahan Latibari, M. Mehrali, S.N. Kazi, C.S. Oon, et al., Experimental investigation of convective heat transfer using graphene nanoplatelet based nanofluids under turbulent flow conditions, Ind. Eng. Chem. Res. 53 (2014) 12455–12465.

[22] M.M. Heyhat, S. Kimiagar, N. Ghanbaryan Sani Gasem Abad, E. Feyzi, Thermal conductivity of reduced graphene oxide by pulse laser in ethylene glycol, Phys. Chem. Res. 4 (2016) 407–415.

[23] S.R. Kimiagar Nasim, Thermal conductivity of nanofluids containing microwave hydrothermal reactor reduced graphene oxide nanosheets, High Temp. – High Pressures 46 (2017) 35–43.

[24] D. Cabaleiro, L. Colla, S. Barison, L. Lugo, L. Fedele, S. Bobbo, Heat transfer capability of (Ethylene Glycol + Water)-based nanofluids containing graphene nanoplatelets: design and thermophysical profile, Nanoscale Res. Lett. 12 (2017) 53.

[25] R. Ranjbarzadeh, A.H. Meghdadi Isfahani, M. Afrand, A. Karimipour, M. Hojaji, An experimental study on heat transfer and pressure drop of water/graphene oxide nanofluid in a copper tube under air cross-flow: applicable as a heat exchanger, Appl. Therm. Eng. 125 (2017) 69–79.

[26] R. Ranjbarzadeh, A. Karimipour, M. Afrand, A.H.M. Isfahani, A. Shirneshan, Empirical analysis of heat transfer and friction factor of water/graphene oxide nanofluid flow in turbulent regime through an isothermal pipe, Appl. Therm. Eng. 126 (2017) 538–547.

[27] M.N.A.W.M. Yazid, N.A.C. Sidik, W.J. Yahya, Heat and mass transfer characteristics of carbon nanotube nanofluids: a review, Renew. Sustain. Energy Rev. 80 (2017) 914–941.

[28] N.A.C. Sidik, M.N.A.W.M. Yazid, S. Samion, A review on the use of carbon nanotubes nanofluid for energy harvesting system, Int. J. Heat Mass Transf. 111 (2017) 782–794.

[29] E.-O.-l. Ettefaghi, A. Rashidi, B. Ghobadian, G. Najafi, M.H. Khoshtaghaza, N.A.C. Sidik, et al., Experimental investigation of conduction and convection heat transfer properties of a novel nanofluid based on carbon quantum dots, Int. Commun. Heat Mass Transf. 90 (2018) 85–92.

[30] J.P. Meyer, M. Everts, Single-phase mixed convection of developing and fully developed flow in smooth horizontal circular tubes in the laminar and transitional flow regimes, Int. J. Heat Mass Transf. 117 (2018) 1251–1273.

[31] A. Albojamal, K. Vafai, Analysis of single phase, discrete and mixture models, in predicting nanofluid transport, Int. J. Heat Mass Transf. 114 (2017) 225–237.

[32] V. Bianco, F. Chiacchio, O. Manca, S. Nardini, Numerical investigation of nanofluids forced convection in circular tubes, Appl. Therm. Eng. 29 (2009) 3632–3642.

[33] A. Ijam, R. Saidur, P. Ganesan, A. Moradi Golsheikh, Stability, thermo-physical properties, and electrical conductivity of graphene oxide-deionized water/ethylene glycol based nanofluid, Int. J. Heat Mass Transf. 87 (2015) 92–103.

[34] S.M. Vanaki, P. Ganesan, H.A. Mohammed, Numerical study of convective heat transfer of nanofluids: a review, Renew. Sustain. Energy Rev. 54 (2016) 1212–1239.

[35] B.C. Pak, Y.I. Cho, Hydrodynamic and heat transfer study of dispersed fluids with submicron metallic oxide particles, Exp. Heat Transfer 11 (1998) 151–170.

[36] V. Kumar, A.K. Tiwari, S.K. Ghosh, Application of nanofluids in plate heat exchanger: a review, Energy Convers. Manage. 105 (2015) 1017–1036.

[37] R. American Society of Heating and E. Air-Conditioning, 2005 ASHRAE Handbook: Fundamentals – SI edition. Atlanta, Ga.: American Society of Heating Refrigerating and Air-Conditionin, 2005.

[38] S.W. Churchill, H. Ozoe, Correlations for laminar forced convection with uniform heating in flow over a plate and in developing and fully developed flow in a tube, J. Heat Transfer 95 (1973) 78–84.

[39] C.O. Popiel, J. Wojtkowiak, Simple formulas for thermophysical properties of liquid water for heat transfer calculations (from 0°C to 150°C), Heat Transfer Eng. 19 (1998) 87–101.

[40] I.D. Garbadeen, M. Sharifpur, J.M. Slabber, J.P. Meyer, Experimental study on natural convection of MWCNT-water nanofluids in a square enclosure, Int. Commun. Heat Mass Transfer 88 (2017) 1–8.

[41] A. Ghozatloo, A. Rashidi, M. Shariaty-Niassar, Convective heat transfer enhancement of graphene nanofluids in shell and tube heat exchanger, Exp. Therm Fluid Sci. 53 (2014) 136–141.

[42] H.K. Arzani, A. Amiri, S.N. Kazi, B.T. Chew, A. Badarudin, Experimental and numerical investigation of thermophysical properties, heat transfer and pressure drop of covalent and noncovalent functionalized graphene nanoplatelet-based water nanofluids in an annular heat exchanger, Int. Commun. Heat Mass Transfer 68 (2015) 267–275.

[43] A.O. Cárdenas Gómez, A.R.K. Hoffmann, E.P. Bandarra Filho, Experimental evaluation of CNT nanofluids in single-phase flow, Int. J. Heat Mass Transf. 86 (2015) 277–287.